Biochemical and Biophysical Research Communications 495 (2018) 1028–1033

Contents lists available at ScienceDirect

Biochemical and Biophysical Research Communications

journal homepage: www.elsevier.com/locate/ybbrc

Temporally coordinated spiking activity of human induced pluripotent stem cell-derived neurons co-cultured with astrocytes

Tasuku Kayama [a], Ikuro Suzuki [b, *], Aoi Odawara [b, c], Takuya Sasaki [a, d, **], Yuji Ikegaya [a, e]

[a] Laboratory of Chemical Pharmacology, Graduate School of Pharmaceutical Sciences, The University of Tokyo, 7-3-1 Hongo, Bunkyo-ku, Tokyo, 113-0033, Japan
[b] Department of Electronics, Graduate School of Engineering, Tohoku Institute of Technology, 35-1 Yagiyama Kasumicho, Taihaku-ku, Sendai, Miyagi, 982-8577, Japan
[c] Japan Society for the Promotion of Science, 5-3-1 Koujimachi, Chiyoda-ku, Tokyo, 102-0083, Japan
[d] Precursory Research for Embryonic Science and Technology, Japan Science and Technology Agency, 4-1-8 Honcho, Kawaguchi, Saitama, 332-0012, Japan
[e] Center for Information and Neural Networks, Suita City, Osaka, 565-0871, Japan

ARTICLE INFO

Article history:
Received 10 November 2017
Accepted 18 November 2017
Available online 21 November 2017

Keywords:
Astrocyte co-culture
Human induced-pluripotent stem cell-derived neurons
Synchronization
Multi-electrode array

ABSTRACT

In culture conditions, human induced-pluripotent stem cells (hiPSC)-derived neurons form synaptic connections with other cells and establish neuronal networks, which are expected to be an *in vitro* model system for drug discovery screening and toxicity testing. While early studies demonstrated effects of co-culture of hiPSC-derived neurons with astroglial cells on survival and maturation of hiPSC-derived neurons, the population spiking patterns of such hiPSC-derived neurons have not been fully characterized. In this study, we analyzed temporal spiking patterns of hiPSC-derived neurons recorded by a multi-electrode array system. We discovered that specific sets of hiPSC-derived neurons co-cultured with astrocytes showed more frequent and highly coherent non-random synchronized spike trains and more dynamic changes in overall spike patterns over time. These temporally coordinated spiking patterns are physiological signs of organized circuits of hiPSC-derived neurons and suggest benefits of co-culture of hiPSC-derived neurons with astrocytes.

1. Introduction

Human induced-pluripotent stem cells (hiPSCs) have been differentiated into central nerve cells [1–3], which have been expected to be invaluable tools for stem cell-based transplantation therapy and disease modeling [4,5]. Furthermore, a culture system of hiPSC-derived neurons have been now applied to drug discovery screening and toxicity testing [6,7].

A number of studies have now reported that hiPSC-derived neurons *in vitro* can form functional synaptic connections with other neurons and establish intricate neuronal networks [2,7–9]. Electrophysiological studies have demonstrated that such hiPSC-derived neuronal populations cultivated on glass dishes can emit synchronized spikes [7,10,11], implying that these neurons are successfully differentiated and incorporated into functional neuronal circuits by forming synaptic contacts with other neurons, similar to neurons in the central nervous system.

Co-culture of hiPSC-derived neurons with astroglial cells, rather than culture of hiPSC-derived neurons alone, has been shown to promote maturation of hiPSC-derived neurons, leading to pronounced increases in their survival rates [7,10,12,13], which is in accordance with the possible roles of astrocytes in the development of neuronal networks in the brain [14–16]. Consistently, hiPSC-derived neurons co-cultured with astrocytes exhibit higher frequencies of burst spikes and a larger number of synchronized population spikes [7,10].

While co-culture with astrocytes has been shown to maintain and elevate overall activity levels of hiPSC-derived neurons, the detailed functional dynamics of hiPSC-derived neurons remain unclear, including (1) whether there are specific sets of hiPSC-

Abbreviation: hiPSC, human induced-pluripotent stem cell; N culture, neuron culture; N-A co-culture, neuron-astrocyte co-culture; ISI, inter-spike interval.

* Corresponding author. Department of Electronics, Graduate School of Engineering, Tohoku Institute of Technology, 35-1 Yagiyama Kasumicho, Taihaku-ku, Sendai, Miyagi, 982-8577, Japan.

** Corresponding author. Laboratory of Chemical Pharmacology, Graduate School of Pharmaceutical Sciences, The University of Tokyo, 7-3-1 Hongo, Bunkyo-ku, Tokyo, 113-0033, Japan.

E-mail addresses: i-suzuki@tohtech.ac.jp (I. Suzuki), tsasaki@mol.f.u-tokyo.ac.jp (T. Sasaki).

https://doi.org/10.1016/j.bbrc.2017.11.115
0006-291X/

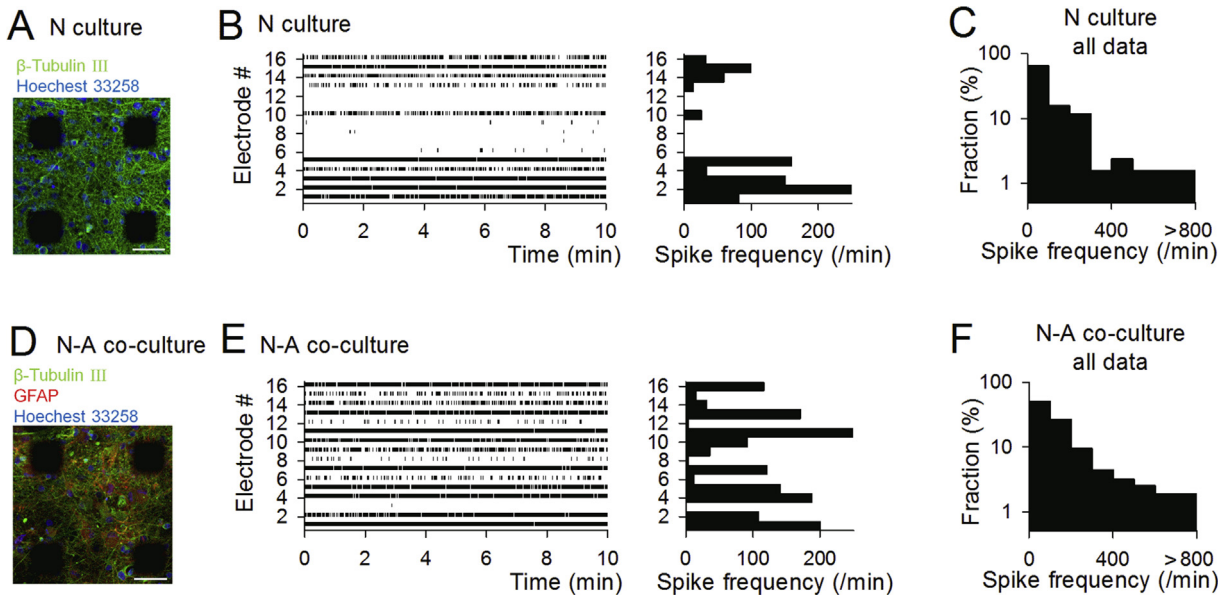

Fig. 1. Basic characteristics of hiPSC-derived neuron spiking activity recorded by the MEA system. (A) A representative image of immunohistochemistry of hiPSC-derived neurons labeled with anti-β-tublin III (green, neuronal marker) and Hoechest 33258 (blue, nuclear marker) antibodies cultivated on an MEA chip (N culture). Scale bar = 50 μm. (B) (Left) A rastergram showing spiking activity patterns detected by 16 electrodes in a N culture dish. Each row represents a single electrode, and each dot represents a single spike. (Right) The spike frequencies of the individual electrodes, corresponding to the left raster plot. (C) The distribution of the percentage of spike frequency in all N culture data (n = 128 electrodes from 8 dishes). (D) A representative image of immunohistochemistry of hiPSC-derived neurons cultured with astrocytes (N-A co-culture). Cells were labeled with anti-β-tublin III (green), GFAP (red, astrocyte marker), and Hoechest 33258 (blue) antibodies. Scale bar = 50 μm. (E and F) Same as in B and C but for N-A co-culture (n = 160 electrodes from 10 dishes).

derived neurons that exhibit synchronized spikes, (2) whether co-culture with astrocytes affects these coordinated temporal patterns, and (3) how stably such spike patterns are maintained over time. To address these questions, we analyzed the temporal spiking patterns of hiPSC-derived neurons recorded by a multi-electrode array (MEA) system. The recording system enables non-invasive, real-time, multi-point measurement of the activity of cultured neurons as previously reported [7,11]. We found that co-culture of hiPSC-derived neurons with astrocytes induced more prominent synchronized spikes of subsets of neurons and larger dynamic changes in their net activity patterns than culture of hiPSC-derived neurons alone.

2. Material and methods

2.1. Culture of hiPSC-derived cerebral cortical neurons

Human induced PSC-derived cortical neurons (XCL-1, XCell Science Inc., USA) were cultured at 3.0×10^5 cells/cm^2 on 16-channel per well across 24 wells MEA plate (Alpha Med Scientific) coated with Polyethyleneimine (Sigma) and Laminin-511 (Nippi). For culture on MEAs, Neural medium (XCell Science) with supplement A (Xcell Science) and 100 U/mL penicillin/streptomycin (168-23191, Wako) was used for 8 days. After 8 days culture, medium was replaced to BrainPhys Neuronal Medium with SM 1 neuronal supplement (STEMCELL technologies, USA). Human iPSC-derived astrocytes (XCL-1, XCell Science) were seeded at 3.0×10^4 cells per well. Half of the media was exchanged every 4 days.

2.2. Extracellular recording

Spontaneous firings were acquired at 37 °C under a 5% CO_2 atmosphere using a 24 wells MEA system (Presto; Alpha Med Scientific) at a sampling rate of 20 kHz/channel. Signals were low-pass filtered at 1 kHz and stored on a personal computer.

2.3. Immunohistochemistry

Sample cultures were fixed with 4% paraformaldehyde in phosphate-buffered saline (PBS) on ice (4 °C) for 10 min, followed by methanol on ice (−20 °C) for 10 min. Fixed cells were incubated with 0.2% Triton X-100 in PBS for 5 min, followed by preblock buffer (0.05% Triton-X and 5% goat serum in PBS) at 4 °C for 1 h, and finally with preblock buffer containing a specific primary antibody (1:1000) at 4 °C for 24 h. The primary antibodies used were rabbit anti-β-tubulin III (T2200, Sigma–Aldrich) for the specific labeling of neurons and goat anti-GFAP (ab53554, Abcam). Immunolabeling was visualized by incubation in an appropriate secondary antibody (anti-rabbit 488 Alexa Fluor (A21206, Thermo Fisher Scientific) and anti-goat 680 Alexa Fluor (ab175776, Abcam), 1:1000 in preblock buffer) for 1 h at room temperature. Cell nuclei were counterstained using 1 μg/ml Hoechst 33258 for 1 h at room temperature. Stained cultures were washed twice in preblock buffer (5 min/wash), rinsed twice using PBS, and viewed using a confocal microscope (TCS SP8, Leica).

2.4. Data analyses

Electrophysiological activity was analyzed using MATLAB. In each electrode, a spike of an electrode was detected when the amplitude of a negative deflection of extracellularly recorded signal exceeded a threshold of 10 μV, which corresponds to approximately 5 standard deviations of the baseline noise during quiescent periods. Negative deflections with a maximal first derivative of less than 3.5 μV/ms were regarded as false-positive signals and excluded from spike signals. Synchronized spikes in the 16 electrodes were computed with a 100-ms bin size. A randomized surrogate dataset was constructed from a real dataset by shuffling inter-spike intervals (ISIs) in each electrode. Cross-correlograms

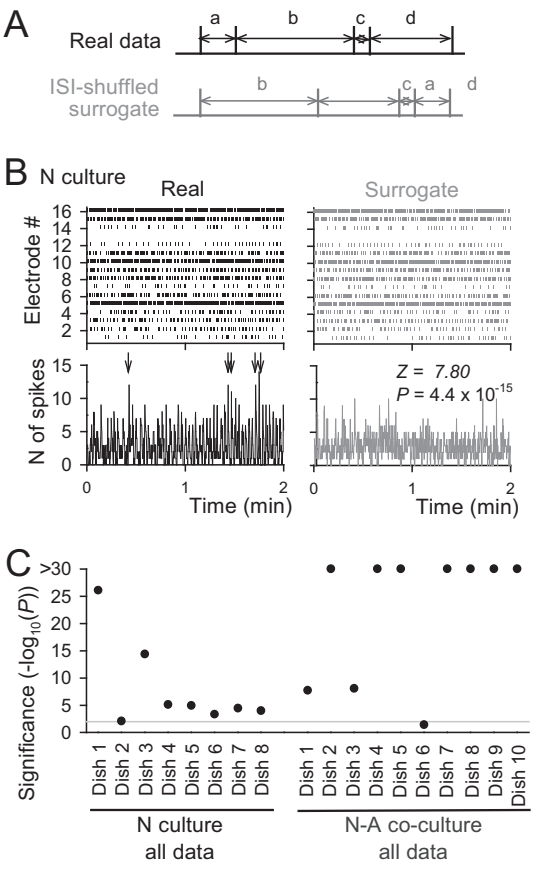

Fig. 2. Synchronized activity of hiPSC-derived neuronal populations. (A) To collate the event correlations between neurons, the inter-spike intervals (ISIs) were transposed at random within an electrode. (B) A representative rastergram of 16 electrodes from a dish in N culture (left) was ISI-shuffled to create a surrogate dataset (right). The bottom panels show the number of spikes every 100-ms bin. The arrows above represent synchronized activity of more than 10 spikes. The distribution of the number of spikes in the original dataset ($n = 6000$ bins) was compared to that in the corresponding 10 surrogates ($n = 60000$ bins), showing a significant difference between the two variables ($Z = 7.80$, $P = 4.4 \times 10^{-15}$, Wilcoxon rank-sum test). (C) The same analysis was applied to all datasets, and statistical significance ($-\log_{10}(P)$) was plotted for individual dishes. The horizontal gray line indicates $P = 0.01$, corresponding with significance = 2. N-A culture had significantly larger P values than N culture ($P = 0.0117$, Wilcoxon rank-sum test).

between two neurons were computed with a time window of 100 ms. Correlational changes between two variables were evaluated by computing a Pearson correlation coefficient. All data are expressed as the mean ± standard error of the mean (SEM).

3. Results

3.1. Recording of spiking activity of cultured hiPSC-derived neurons

Human iPSC-derived neurons were cultured without and with astrocytes, termed as N (neuron only) culture and N-A (neuron-astrocyte) co-culture, respectively, on an MEA chip equipped with 16 recording electrodes (Fig. 1A and D). Representative spontaneous spiking patterns of hiPSC-derived neurons detected in each culture condition are shown as raster plots in Fig. 1B (N culture) and Fig. 1E (N-A co-culture). During an observation period of 10 min, 86.7% and 94.4% of the electrodes had at least one spikes (i.e., non-silent electrodes), and single non-silent electrodes exhibited 103.9 ± 18.0 spikes min^{-1} (median = 26.6 min^{-1}) and 122.2 ± 15.3 spikes min^{-1} (median = 53.9 spikes min^{-1}) in N culture and N-A co-culture, respectively (Fig. 1C and F; N culture: $n = 8$ dishes; N-A co-culture $n = 10$ dishes), demonstrating that a larger number of hiPSC-derived neuronal spikes were observed in N-A co-culture than in N culture. These results are consistent with previous observations that co-culture of astrocytes with hiPSC-derived neurons facilitate maturation of neuronal networks, making hiPSC-derived neurons highly active [7,10].

3.2. Synchronized activity of hiPSC-derived neuronal populations

Population spiking patterns of hiPSC-derived neurons were analyzed (Fig. 2). In an example 10-min window of recording data obtained from a single dish shown in Fig. 2B on the left, 16 electrodes detected 2.86 spikes on average in any given 100-ms bin. In addition, the neuronal populations occasionally exhibited large synchronized events as indicated by the arrows. To quantify whether a stochastic process could account for such large neuronal synchronized events, the original raster plot was compared with raster plots of surrogate datasets in which inter-spike intervals (ISIs) were randomly shuffled in each non-silent electrode (an example shown in Fig. 2B right). This shuffling procedure randomized the temporal correlation of spikes across multiple electrodes without altering the total spike counts (Fig. 2A). For each original raster plot, 10 surrogates were created, and the probability distribution of spike counts observed in 100-ms bins was compared between the original raster plot and the corresponding 10 surrogate raster plots. In the example raster plot shown in Fig. 2B, the distribution was significantly different between the two datasets revealed by a Wilcoxon rank-sum test ($Z = 7.80$, $P = 4.4 \times 10^{-15}$). Specifically, a large synchronization including more than 10 spikes emerged at a frequency of 6.6 min^{-1} in the real datasets, while such synchronization rarely occurred in the surrogates (0.3 min^{-1}). The same analysis was applied to all datasets and is summarized in Fig. 2C, showing that similar significant differences at a significance level of 1% ($P < 0.01$) were observed, except in Dish 6 in N-A culture. These results suggest that synchronization of hiPSC-derived neurons could not be simply accounted for by chance. Notably, the significance, computed as $-\log_{10}(P)$, was higher in N-A culture than in N culture ($P = 0.0117$, Wilcoxon rank-sum test). The results suggest that co-culture of astrocytes with hiPSC-derived neurons further facilitates organized activity of hiPSC-derived neurons.

3.3. Pairwise synchronization of hiPSC-derived neurons

Detailed synchronized spike patterns were characterized by analyzing pairwise synchronization between two electrodes. In each pair of non-silent electrodes, the number of synchronized spikes (N_{sync}) in a 10-min recording period was compared with those of 100 surrogate datasets that were constructed as described for Fig. 2A (Fig. 3A). To quantify the significance of the pairwise synchronization, a N_{sync} of a real dataset was converted to a z score based on the mean and standard deviation of the distribution of the N_{sync} of the corresponding 100 surrogate datasets (Fig. 3A, right). A highly synchronized electrode pair was defined if the z score was more than 1.96, which represents a significance level of $P < 0.05$ (Fig. 3B). In N culture and N-A co-culture, the proportion of highly synchronized pairs of all possible active electrode pairs was 39.2% (259 out of 661 pairs) and 57.1% (588 out of 1030 pairs), respectively ($\chi^2 = 51.3$, $^*P = 4.1 \times 10^{-13}$, chi-square test). Overall, the distribution of z scores in N-A co-culture (median = 2.73) was significantly different from that in N culture (median = 1.30) ($Z = 8.67$, $P = 4.3 \times 10^{-8}$, Wilcoxon rank-sum test), again confirming that N-A co-culture exhibited more synchronized spikes across electrodes.

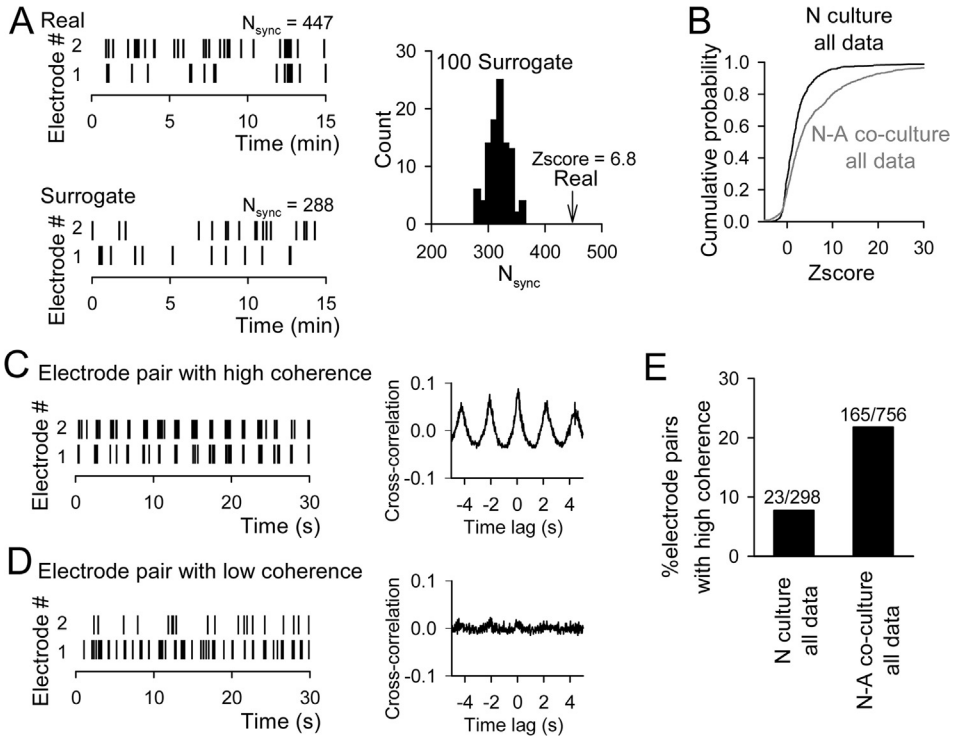

Fig. 3. Pairwise synchronization of hiPSC-derived neurons. (A) (Left) Spike patterns of a representative two electrodes (top). Each vertical line represents each spike. The number of synchronized spikes (N_{sync}) was counted within a 100-ms time window. A typical surrogate dataset was generated from the real dataset as in Fig. 2A (bottom). (Right) For this electrode pair, a real N_{sync} value is indicated by the arrow, which was compared with the distribution of N_{sync} computed from the corresponding 100 surrogate datasets (gray histogram). Based on the distribution of the surrogate datasets, the z score of the real data was computed to be 6.8. (B) Cumulative distribution of z scores computed in each pair of non-silent electrodes (N culture: $n = 661$ electrode pairs from 8 dishes; N-A co-culture: $n = 1030$ electrode pairs from 10 dishes). Electrode pairs with z scores greater than 1.96 were defined as highly synchronized electrode pairs. $Z = 8.67$, $P = 4.3 \times 10^{-8}$, Wilcoxon rank-sum test. (C, D) Oscillatory spike synchronization of hiPSC-derived neurons. (Left) An example raster plot obtained from two active electrodes showing high (C) and low (D) coherent synchronized spikes. (Right) The cross-correlograms of spiking activity constructed from the two electrodes with a time window of 200 ms. (E) The percentage of electrode pairs with high coherence out of all active electrode pairs. $\chi^2 = 29.0$, $^*P = 3.7 \times 10^{-8}$, chi-square test.

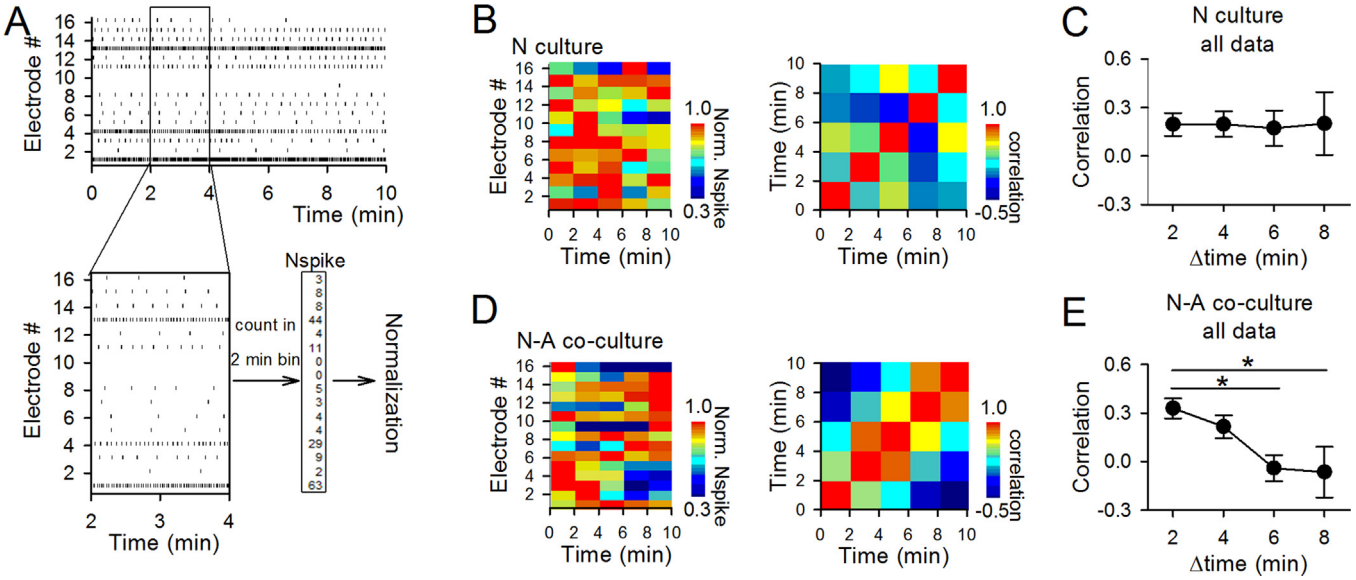

Fig. 4. Temporal changes in spontaneous activity patterns of hiPSC-derived neurons. (A) An example rastergram of 16 electrodes. Spikes in a 2-min time window (shown by boxed area) were counted, normalized for each non-silent electrode and converted to a vector ***s***. (B) (Left) A series of 2-min vectors were combined to represent a 10-min recording window obtained from a N culture dish, shown as a pseudo-color image. (Right) The correlation matrix computed for all possible pairs in the 2-min time bins. (C) Correlation coefficients of all datasets in N culture were averaged for each time difference. No significant difference was found across time. One-way ANOVA, $F(3,79) = 0.01$, $P = 0.99$. (D) Same as in B but for a N-A co-culture dish. (E) Same as in C but for N-A co-culture. A significant decrease in the coefficient was found depending on the time difference. Error bars are SEM. $^*P < 0.05$, Tukey's test followed by one-way ANOVA. (For interpretation of the references to colour in this figure legend, the reader is referred to the web version of this article.)

3.4. Oscillatory spike synchrony of hiPSC-derived neurons

The temporal patterns of pairwise synchronized spikes were further analyzed by computing the cross-correlation of pairs of electrodes with more than 10 spikes min^{-1}, termed active electrodes. Fig. 3C–D shows representative pairs of active electrodes; the top panel represents an active electrode pair with high coherence showing oscillatory synchronized activity at a cycle of several seconds, whereas the bottom panel represents an active electrode pair with low coherence, showing no such prominent coherence. The cross-correlogram was computed from each active electrode pair as shown in the right panels. If correlation coefficients were higher than 10 standard deviations (SDs) above the mean of the bottom 50% of all coefficients, the electrode pair was regarded to have high coherence of spiking activity. Of the 298 and 756 active electrode pairs tested, 23 and 165 (7.7% and 21.8%) pairs were judged to be pairs with high coherence in N culture and N-A co-culture, respectively (Fig. 3E). The proportion of electrode pairs with high coherence in N-A co-culture was significantly higher than that in N culture ($\chi^2 = 29.0$, $^*P = 3.7 \times 10^{-8}$, chi-square test), suggesting that co-culture with astrocytes increased the oscillatory and highly coherent spiking patterns of hiPSC-derived neurons. The average time lag giving the second maximum coefficients in the cross-correlograms was 1.99 ± 0.03 s ($n = 188$ electrode pairs).

3.5. Temporal changes in activity states of hiPSC-derived neurons

Finally, we assessed how the activity states of hiPSC-derived neurons change over time. Spike frequencies of all non-silent electrodes in a 2-min time window were counted for every 2 min and converted to a vector $\boldsymbol{s}$ (Fig. 4A). A vector component was normalized by the maximum component of five vector series in each non-silent electrode. Representative pseudo-color images of a series of five consecutive vectors consisting of normalized spike frequencies in a 10-min recording session are shown in Fig. 4B and D left. Pearson correlation coefficients of vectorized spike frequencies were computed between all pairs of 2-min bins as summarized as a correlation matrix (Fig. 4B and D, right). To compute whether spike activity patterns changed over time, the average correlation coefficients were plotted as a function of the time difference (Δtime) for all possible 2-min bins in all datasets (Fig. 4E and F). In N culture, no significant differences in the coefficients were detected across time (Fig. 4C; one-way ANOVA; $F(3,79) = 0.01$, $P = 0.99$). On the other hand, in N-A co-culture, the correlation coefficients decreased as the time difference increased, and significant differences were observed between a time difference of 2 min and time differences of 6 min and 8 min (Fig. 4E; $P < 0.05$, Tukey's test followed by one-way ANOVA; $F(3,99) = 5.36$, $P = 0.0019$). These results demonstrate that the activity patterns of hiPSC-derived neuronal populations in N-A co-culture changed over time more than those in N culture.

4. Discussion

In this study, we analyzed spike patterns of hiPSC-derived neurons obtained from an MEA recording system. Compared with the features in hiPSC-derived neurons in N culture, several neurophysiological features appeared in hiPSC-derived neurons co-cultured with astrocytes: (1) larger spike synchronization of neuronal populations, (2) more and more highly coherent synchronized spikes between specific neuronal populations, and (3) larger changes in population spike patterns of hiPSC-derived neurons over time.

Our finding of synchronized spikes of hiPSC-derived neuronal populations is a partial replication of the previous findings of synchronized spike bursts of hiPSC-derived neurons [7,11]. Our study extended these early findings by showing that specific neuronal groups in neuron-astrocyte co-culture can exhibit more frequent synchronized spikes, and some of these synchronized events are time-locked to oscillatory rhythms, both of which are a physiological sign of well-organized neuronal networks. These findings suggest that co-culture with astrocytes not only elevates the overall excitability of hiPSC-derived neurons but also facilitates maturation of synaptic connections between specific hiPSC-derived neurons, leading to the formation of functional neuronal circuits derived from hiPSCs. Several mechanisms have been suggested to explain the increased maturation of neurons by astrocytes, including axonal elongation, branching, synaptic formation, and maturation [14–16]. Moreover, astrocytes can maintain and even potentiate neurotransmission at matured synapses [17–19]. A combination of these mechanisms of neuron-astrocyte interactions likely facilitate and stabilize functional circuits of hiPSC-derived neurons.

Our finding of larger changes in spike patterns of hiPSC-derived neurons over time in N-A culture suggests that these neurons have the ability to generate expanded repertoires of organized spike patterns, which may increase the capacity of memory and information processing in the neuronal networks [20,21]. Developmentally, while the exact functional significance of such time-varying neuronal activity remains unclear, it implies that hiPSC-derived neurons are subject to a larger variety of types of activity-dependent plasticity, which may contribute to the enrichment of the diversity and capacity of neuronal circuit computation. These positive effects of astrocytes on the maturation of functional hiPSC-derived neuronal networks might be more crucial for long-term cultures [7].

In summary, co-culturing hiPSC-derived neurons and astrocytes gives rise to functional neuronal networks with a wider range of spatiotemporal spiking patterns than culturing hiPSC-derived neurons alone. Such organized and heterogeneous activity patterns are more consistent with highly complicated neuronal networks in the biological brain. Recent studies have suggested that a culture system of hiPSC-derived neurons is as an excellent tool for drug discovery screening and toxicity testing [6,7]. Our present study adds to a growing body of evidence that synchronized spike patterns of hiPSC-derived neurons is applicable as a physiological marker and suggests that such physiological signals can be enriched by combining hiPSC-derived neurons and astrocytes in the culture system.

Acknowledgements

We thank Alpha Med Scientific and XCell Science Company for supporting this research. This work was supported by AMED 17bk0104076h0201 (INCENS: iPS-non clinical experiments for nervous system) and Kaken-hi (17K20111) to I.S and Kaken-hi (17H05939; 17H05551) and the Konica Minolta Science and Technology Foundation to T.S.

Transparency document

Transparency document related to this article can be found online at https://doi.org/10.1016/j.bbrc.2017.11.115.

References

[1] D.V. Hansen, J.L. Rubenstein, A.R. Kriegstein, Deriving excitatory neurons of the neocortex from pluripotent stem cells, Neuron 70 (2011) 645–660.
[2] Y. Shi, P. Kirwan, J. Smith, H.P. Robinson, F.J. Livesey, Human cerebral cortex development from pluripotent stem cells to functional excitatory synapses, Nat. Neurosci. 15 (2012) 477–486. S471.

[3] F. Soldner, J. Laganiere, A.W. Cheng, D. Hockemeyer, Q. Gao, R. Alagappan, V. Khurana, L.I. Golbe, R.H. Myers, S. Lindquist, L. Zhang, D. Guschin, L.K. Fong, B.J. Vu, X. Meng, F.D. Urnov, E.J. Rebar, P.D. Gregory, H.S. Zhang, R. Jaenisch, Generation of isogenic pluripotent stem cells differing exclusively at two early onset Parkinson point mutations, Cell 146 (2011) 318–331.
[4] K. Takahashi, K. Tanabe, M. Ohnuki, M. Narita, T. Ichisaka, K. Tomoda, S. Yamanaka, Induction of pluripotent stem cells from adult human fibroblasts by defined factors, Cell 131 (2007) 861–872.
[5] A.B. Cherry, G.Q. Daley, Reprogrammed cells for disease modeling and regenerative medicine, Annu. Rev. Med. 64 (2013) 277–290.
[6] S.J. Engle, D. Puppala, Integrating human pluripotent stem cells into drug development, Cell Stem Cell 12 (2013) 669–677.
[7] A. Odawara, Y. Saitoh, A.H. Alhebshi, M. Gotoh, I. Suzuki, Long-term electrophysiological activity and pharmacological response of a human induced pluripotent stem cell-derived neuron and astrocyte co-culture, Biochem. Biophys. Res. Commun. 443 (2014) 1176–1181.
[8] J.E. Kim, M.L. O'Sullivan, C.A. Sanchez, M. Hwang, M.A. Israel, K. Brennand, T.J. Deerinck, L.S. Goldstein, F.H. Gage, M.H. Ellisman, A. Ghosh, Investigating synapse formation and function using human pluripotent stem cell-derived neurons, Proc. Natl. Acad. Sci. U. S. A. 108 (2011) 3005–3010.
[9] T. Hiragi, M. Andoh, T. Araki, T. Shirakawa, T. Ono, R. Koyama, Y. Ikegaya, Differentiation of human induced pluripotent stem cell (hiPSC)-Derived neurons in mouse hippocampal slice cultures, Front. Cell. Neurosci. 11 (2017) 143.
[10] K. Fukushima, Y. Miura, K. Sawada, K. Yamazaki, M. Ito, Establishment of a human neuronal network assessment system by using a human neuron/astrocyte Co-Culture derived from fetal neural stem/progenitor cells, J. Biomol. Screen. 21 (2016) 54–64.
[11] A. Odawara, H. Katoh, N. Matsuda, I. Suzuki, Physiological maturation and drug responses of human induced pluripotent stem cell-derived cortical neuronal networks in long-term culture, Sci. Rep. 6 (2016) 26181.
[12] X. Tang, L. Zhou, A.M. Wagner, M.C. Marchetto, A.R. Muotri, F.H. Gage, G. Chen, Astroglial cells regulate the developmental timeline of human neurons differentiated from induced pluripotent stem cells, Stem Cell Res. 11 (2013) 743–757.
[13] Y. Qi, X.J. Zhang, N. Renier, Z. Wu, T. Atkin, Z. Sun, M.Z. Ozair, J. Tchieu, B. Zimmer, F. Fattahi, Y. Ganat, R. Azevedo, N. Zeltner, A.H. Brivanlou, M. Karayiorgou, J. Gogos, M. Tomishima, M. Tessier-Lavigne, S.H. Shi, L. Studer, Combined small-molecule inhibition accelerates the derivation of functional cortical neurons from human pluripotent stem cells, Nat. Biotechnol. 35 (2017) 154–163.
[14] L.E. Clarke, B.A. Barres, Emerging roles of astrocytes in neural circuit development, Nature reviews, Neuroscience 14 (2013) 311–321.
[15] N.J. Allen, M.L. Bennett, L.C. Foo, G.X. Wang, C. Chakraborty, S.J. Smith, B.A. Barres, Astrocyte glypicans 4 and 6 promote formation of excitatory synapses via GluA1 AMPA receptors, Nature 486 (2012) 410–414.
[16] E.G. Hughes, S.B. Elmariah, R.J. Balice-Gordon, Astrocyte secreted proteins selectively increase hippocampal GABAergic axon length, branching, and synaptogenesis, Mol. Cell. Neurosci. 43 (2010) 136–145.
[17] C. Henneberger, T. Papouin, S.H. Oliet, D.A. Rusakov, Long-term potentiation depends on release of D-serine from astrocytes, Nature 463 (2010) 232–236.
[18] M.M. Halassa, P.G. Haydon, Integrated brain circuits: astrocytic networks modulate neuronal activity and behavior, Annu. Rev. Physiol. 72 (2010) 335–355.
[19] T. Sasaki, T. Ishikawa, R. Abe, R. Nakayama, A. Asada, N. Matsuki, Y. Ikegaya, Astrocyte calcium signalling orchestrates neuronal synchronization in organotypic hippocampal slices, J. Physiol. 592 (2014) 2771–2783.
[20] T. Sasaki, N. Matsuki, Y. Ikegaya, Metastability of active CA3 networks, J. Neurosci. 27 (2007) 517–528.
[21] Y. Ikegaya, G. Aaron, R. Cossart, D. Aronov, I. Lampl, D. Ferster, R. Yuste, Synfire chains and cortical songs: temporal modules of cortical activity, Science 304 (2004) 559–564.